Available online at www.sciencedirect.com
ScienceDirect
Trans. Nonferrous Met. Soc. China 26(2016) 2810−2817
Transactions of Nonferrous Metals Society of China
www.tnmsc.cn

Effect of Mg addition on mechanical and thermoelectrical properties of Al−Al_2O_3 nanocomposite

A. WAGIH

Mechanical Design and Production Dept, Faculty of Engineering, Zagazig University, P. O. Box 44519, Zagazig, Sharkia, Egypt

Received 30 November 2015; accepted 27 February 2016

Abstract: The effects of Mg addition on mechanical thermo-electrical properties of Al−Mg/5%Al_2O_3 nanocomposite with different Mg contents (0, 5%, 10% and 20%) produced by mechanical alloying were studied. Scanning electron microscopy analysis (SEM), X-ray diffraction analysis (XRD) and transmission electron microscopy (TEM) were used to characterize the produced powder. The results show that addition of Mg forms a predominant phase (Al−Mg solid solution). By increasing the mass fraction of Mg, the crystallite size decreases and the lattice strain increases which results from the atomic penetration of Mg atoms into the substitutional sites of Al lattice. The microhardness of the composite increases with the increase of the Mg content. The thermal and electrical conductivities increase linearly with the temperature increase in the inspected temperature range. Moreover, the thermal conductivity increases with the increase of Mg content.

Key words: Al−Al_2O_3 nanocomposite; Mg; mechanical alloying; microhardness; thermoelectrical properties

1 Introduction

Metal matrix composites (MMCs) have significantly improved properties such as high specific strength, specific modulus, damping capacity and good wear resistance compared with the unreinforced alloys. Aluminum matrix composites reinforced with particles are widely used for high performance applications such as automotive, military, aerospace and electricity industries because of their improved physical and mechanical properties [1,2]. Owing to low density, low melting point, high specific strength and thermal conductivity of aluminum, a wide variety of reinforcement particulates such as SiC, B_4C, Al_2O_3, AlN, Si_3N_4, TiC, TiO_2, TiB_2 and graphite have been reinforced into it. On the other hand, nano-crystalline matrices strengthened by nano-sized reinforcement are expected to have much better microstructural stabilities and performance than nano-crystalline materials [3] due to the occurrence of strengthening by grain boundary and nanoparticle reinforcements [4−6].

High energy ball milling is a simple and useful technique for attaining a homogeneous distribution of the inert fine particles within a fine grained matrix [7,8]. During ball milling, two essential processes occur, cold welding between different particles and fracturing of the cold welded particles due to high energy collision [9,10]. The cold welding minimizes the diffusion distance between the atoms of the different components. The fracturing of the welded particles impedes the clustering of the particles promoting the transfer of the high ball collision energy to all particles and produces new, clean surfaces without oxide layers accelerating the diffusion [9,11].

Due to the importance of aluminum and its alloys, many researchers perform their researchers on the methods of producing aluminum matrix reinforced with both micro and nano Al_2O_3 hard particles with homogenous distribution of the reinforcement in the matrix [7,8,11−14]. The wettability between the reinforcement and the matrix in Al−Al_2O_3 nanocomposite is very low. However, adding some alloying elements such as Mg, Si, and Mo to this composite may enhance the wettability between the composite components [8,15−17].

Thermal conductivity is affected by various factors such as the matrix microstructure, thermal conductivity of the constituent phases, heterogeneous reinforcement distribution porosity content, and the strength of the

Corresponding author: A. WAGIH; Tel: +20-1061474023; E-mail: ahmedwagih@zu.edu.eg
DOI: 10.1016/S1003-6326(16)64409-6

interfacial between bond matrix and the reinforcement [18]. Aluminum-matrix composites are the most widely reported in the literature, but the effect of adding some alloying elements, which have a positive influence on the wettability between the matrix and reinforcement, on the thermal conductivity have not been studied.

Hence, the main objective of the present work is to study the effect of Mg addition on the microstructural, mechanical properties and thermal conductivity of Al−Al_2O_3 nanocomposite through detailed experimentation. Scan electron microscope (SEM), X-ray diffraction (XRD) analysis and transmission electron microscope (TEM) were used to study the microstructural changes in the composite powders. Microhardness test was used to characterize the mechanical properties of the composite. Finally, high precision micrometer was used to measure the electrical conductivity of the prepared samples.

2 Experimental

Commercial pure Al powder (99.5% purity and 80 μm average particle size), Mg powder (99.8% purity and 50 μm average particle size) and Al_2O_3 powder (99.5% purity and 40 μm size) were used as raw materials for composite preparation. Pure powders were milled to form Al−Mg/5%Al_2O_3 composite with the designed Mg MASS fractions (0, 5%, 10% and 20%) in a Fritsch planetary ball mill, while confined in sealed 250 mL steel containers rotated at 250 r/min for 20 h. The detailed explanation of the milling process is shown in Ref. [10].

The powders produced after milling were investigated by using SEM Model Quanta 250 FEG (field emission gun) attached with EDX unit (energy dispersive X-ray analyses), with accelerating voltage of 30 kV. Morphology, size and particle distribution of the milled powders were examined. The nano-crystalline nature of the high-energy ball-milled powders was confirmed using a JEOL 3010 high-resolution transmission electron microscope (HR-TEM).

X-ray diffraction (XRD) patterns were carried by a Rigaku-DXR 3000 X-ray diffractometer using Cu K_α radiation (λ=0.15406 nm) at 30 kV and 30 mA settings. The crystallite size and lattice strain of milled aluminum powders were estimated by XRD peak broadening using the William−Hall method [19].

The XRD can be used to evaluate the peak broadening with the crystallite size and the lattice strain due to the presence of dislocations in nanocomposites. The average crystallite size (D) was measured by WILLIAMSON and HALL [19]:

$$B\cos\theta=(0.9\lambda)/D+4\varepsilon\sin\theta \quad (1)$$

where β, λ, θ, D and ε are full width at half maximum (FWHM), the wave length, peak position, crystallite size and lattice strain, respectively.

Microhardness measurements were conducted using a Vickers indenter at a load of 250 mN on the powder to determine hardness. Dwell time of 5 s was adopted. For measurement of microhardness, the powder mixtures were cold pressed under 250 MPa. Prior to indentation, the surfaces of the samples were polished using a sequence of increasing grit sand paper followed by a series of diamond pastes. Ten indentations were done for each specimen in different spaces through all the areas of the specimen. The hardness (H) can be calculated from the maximum load (F_m) and the maximum penetration depth (h_m) of the indentation curves as [20]:

$$H=0.03784\frac{F_m}{h_m^2} \quad (2)$$

The milled powders were consolidated by cold uniaxial pressing in a cylindrical rigid die (double action type) at 600 MPa, with zinc stearate ($Zn(C_18H_35O_2)_2$) as a lubricant. The consolidated specimens were cylinders of 20 mm in diameter and 40 mm in height. The consolidated specimens were sintered in a hydrogen atmosphere at 500 °C for 5 h. Sintering was performed in a laboratory electro resistance tube furnace with maximum power 3 kW and thermoregulation 1 °C. The heating and cooling rates were 10 °C/min and 2 °C/min, respectively. Sintered samples were cut with a low velocity diamond cutting wheel in a lathe to cylinders of 10 mm in height with the same diameter for the examination of thermal conductivities of the composites.

The thermal conductivity of the material was calculated through its electrical resistivity. The electrical resistivity of the composite was measured by using high precision micrometer, Omega CL8400 at different temperatures (ranging from 300 to 500 K). Three specimens were tested to ensure the accuracy of the test and the average is plotted. In 1853, FRANZ and WIEDEMANN [21] provided an efficient relation which relates the thermal conductivity of the material and its electrical resistivity. So, if the electrical conductivity is known, the thermal conductivity can be expressed as

$$k=LT\sigma \quad (3)$$

where k is the thermal conductivity, L is the Lorentz number (for composites $L=2.45\times10^{-8}$ W·Ω/K^2), T is the absolute temperature, and σ is the electrical conductivity.

3 Results and discussion

3.1 X-ray diffraction analysis

Figure 1 shows X-ray diffraction patterns of

Al−Mg/5%Al_2O_3 (with different Mg contents of 0, 5%, 10% and 20%) nanocomposite powder milled for 20 h. For Al−Mg/Al_2O_3 powder mixtures characteristics Al, Al$(Mg)_{ss}$ and Al_2O_3 were observed. The intensity of the alumina particles in Al/5%Al_2O_3 is larger than its intensity for Al−Mg/5%Al_2O_3. This is due to the fact that alumina particles are extremely small that they are embedded in the Al−Mg matrix. Alumina particles are very brittle and fractured during milling and become finer. At the same time, Mg peaks disappeared completely, which indicate the formation of the FCC supersaturated Al$(Mg)_{ss}$ due to the Mg atomic penetration into the substitution sites of the Al lattice [22].

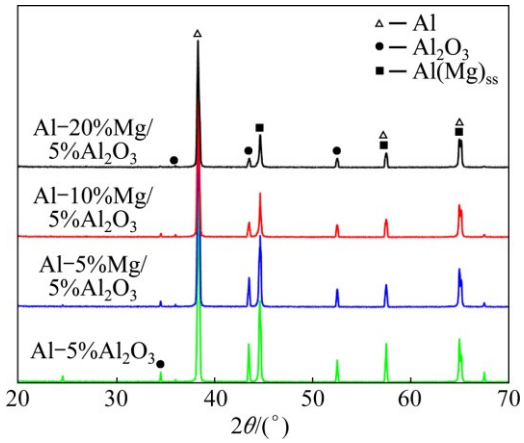

Fig. 1 XRD patterns for Al−Mg/5%Al_2O_3 nanocomposite powder after 20 h milling with different Mg contents (0, 5%, 10% and 20%)

Table 1 shows a clear shift in the 2θ of Al peak at (111) plane to the smaller angle, and peak broadening at the same plane as the Mg content increases. A possible reason for the shift to the smaller angle is the solution of the larger magnesium atoms (Mg atoms have a larger radius than Al atoms) into the Al matrix. Moreover, the broadening of the Al$(Mg)_{ss}$ peaks and decreasing intensities reveal crystallite refinement and accumulation of heterogeneous strain.

Table 1 Comparison of 2θ and FWHM of Al peak at (111) plane

Mg content/%	2θ of Al peak at (111) plane/(°)	FWHM of Al peak at (111) plane/(°)
0	38.421	0.251
5	38.417	0.262
10	38.398	0.278
20	38.375	0.311

Figure 2 shows the effect of Mg content on the crystallite size and lattice strain of examined powder particles. It is observed that increasing Mg content leads to the decrease of the crystallite size, it diminishes from 43 nm without Mg to 26 nm at 20% Mg. This can be related to the fact that as the Mg content increases in the solid solution, the dislocation density increases and leads to the grain refinement [11,23]. Moreover, higher diffusion rate of Mg atoms into deformed Al crystals results from the higher dislocation density. This results in more work hardening effects and smaller crystallite size [11]. On the other hand, the lattice strains are observed with increasing Mg content from 0.22% without Mg to 0.325% for 20% Mg. During milling process, plastic deformations of powder particles lead to increase in crystal defects such as point defects and dislocations [13]. This point defects increase the internal energy and the lattice strain. The dislocations rearrange themselves to a lower energy state leading to the formation of low angle sub-boundaries. At longer time of milling (20 h), due to the higher plastic deformation and generation of more dislocations, the disorientations between sub-grains at their boundaries increase and eventually they turn into high angle boundaries and become grains with nano-scale sizes.

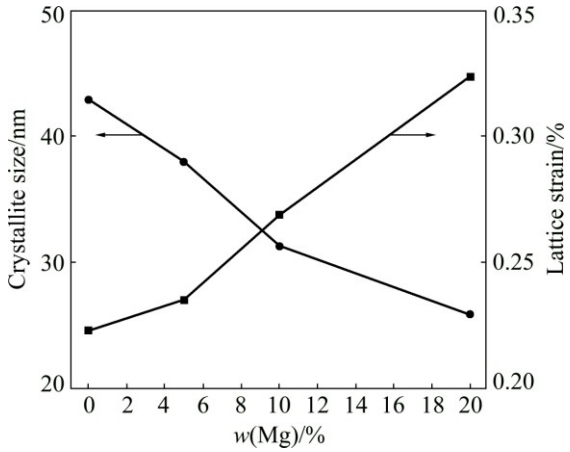

Fig. 2 Effect of Mg content on crystallite size and lattice strain of Al−Mg/5% Al_2O_3 nanocomposite powder after 20 h milling

The first five Al reflections were used to construct a linear plot of $\beta\cos\theta$ against $4\sin\theta$. Considering the isotropic nature of the crystal, the material properties are independent of the direction. Figure 3 shows the W−H analysis for Al−Mg/5%Al_2O_3 nanocomposite with different Mg contents after 20 h milling. From this figure, it is shown that with increasing Mg content, the intercept shifted to higher value, implying that the crystallite size decreases and the corresponding slope of the fit decreases slightly meaning that the lattice strain increases.

3.2 Morphology and particle size distribution

Figure 4 shows the morphology of Al−Mg/5%Al_2O_3 nanocomposite powder after 20 h milling with different

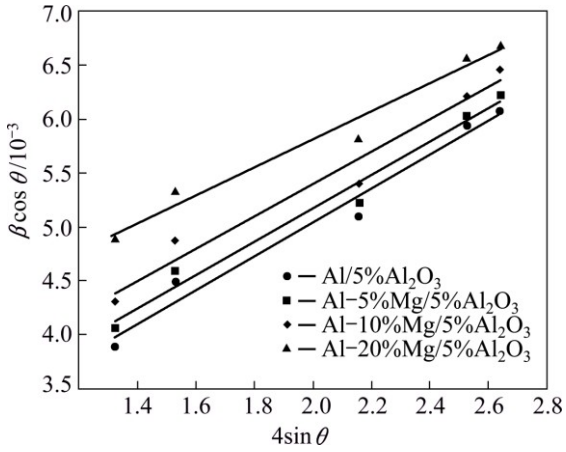

Fig. 3 W−H analysis of Al−Mg/5%Al_2O_3 nanocomposite powder after 20 h milling

Mg contents (0, 5%, 10% and 20%). Figure 4(a) shows the SEM image of Al/5%Al_2O_3. It is noticeable that the matrix particles have flake shape and the average particle size is around 30 μm. By adding 5% Mg to the composite, the particles start to take a spherical shape and the particle size diminishes to 15 μm, as shown in Fig. 4(b). With increasing the Mg content, the particles size decreases and becomes more rounded in its shape. The average particle size reaches 5 μm at 20% Mg composite, as shown in Fig. 4(d). The reason for this phenomenon is the penetration of Mg atoms into the substitutional sites of Al lattice. Additionally, the increase in the defect density and the raise in the temperature caused by the milling process at the Al and Mg interfaces facilitate the diffusion of Mg atoms in the Al matrix. It is important to highlight that, Al−Mg matrix is more brittle than the Al matrix due to the existence of hard Mg atoms and the formation of Al−Mg solid solution ($Al(Mg)_{ss}$), which accelerates fracture action of particles and in its role, reduces not only the matrix particle size but also the reinforcement crystallite size.

Comparing Figs. 4(c) and (d), the reduction rate in the particle size became slower which indicates that mechanical alloying process has become a steady state; by cold working of particles, the welding and fracturing processes have become balanced. That gives evidence on the uniform distribution of the reinforcement in the Al−Mg matrix. So, the mechanical milling process can be accelerated by increasing the Mg content in the composite which reduces the milling time required to reduce the particle size.

Figure 5 shows the TEM images of Al−20%Mg/5% Al_2O_3 nanocomposite powder after 20 h milling. The white dots in the figure represent the reinforcement (Al_2O_3 nano particles). The size of Al_2O_3 nanoparticles

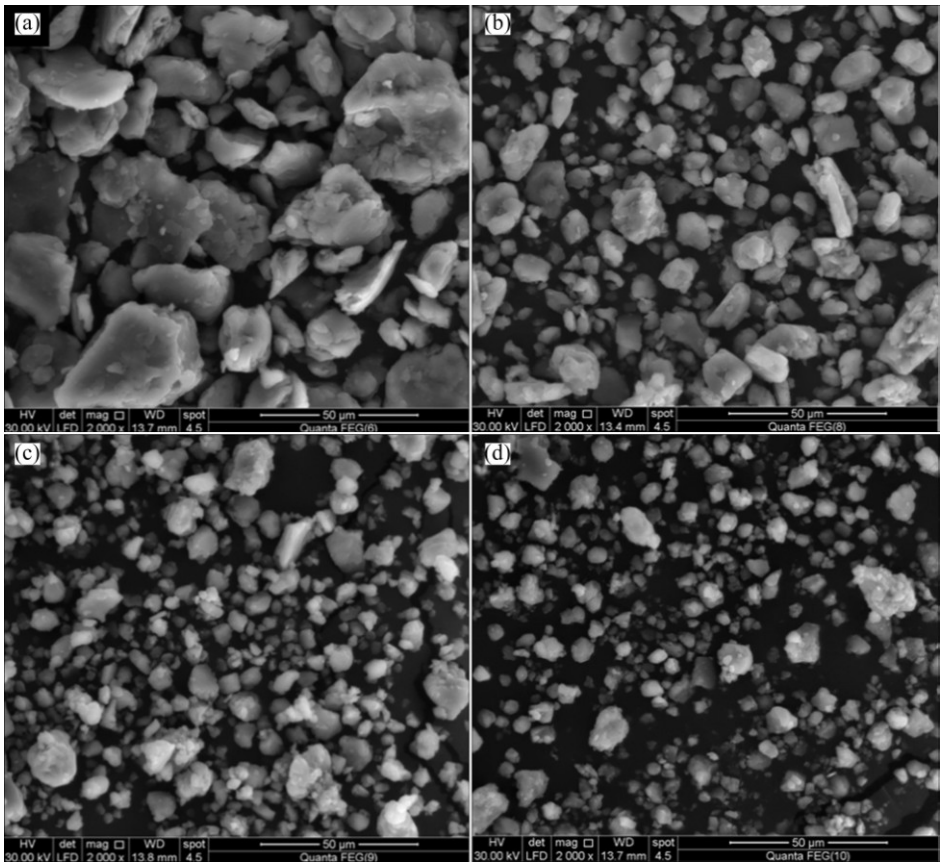

Fig. 4 SEM images of Al−Mg/5%Al_2O_3 nanocomposite powder after 20 h milling: (a) Without Mg; (b) 5% Mg; (c) 10% Mg; (d) 20% Mg

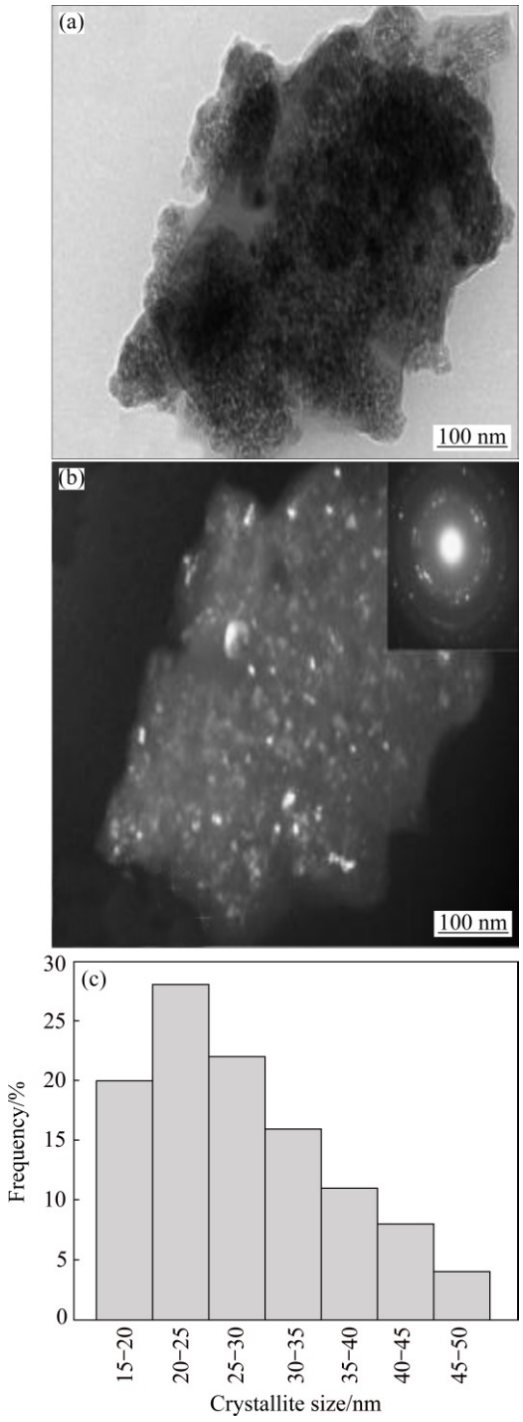

Fig. 5 TEM micrographs of Al−20Mg/5%Al_2O_3 nanocomposite powder after 20 h milling: (a) Bright field image (BFI); (b) Dark field image (DFI) (inset shows the SAD); (c) Crystallite size distribution

ranges from 15 to 50 nm and most of the powders are between 20 and 30 nm in particle size, as seen in Fig. 5(c).

3.3 Microhardness

The effect of fraction of Mg on the microhardness of Al−Mg/5%Al_2O_3 nanocomposite powders milled for 20 h is shown in Fig. 6. Adding 5% Mg to the composite increases its hardness form HV 140 to HV 177. Then, by increasing the Mg content to 10%, the hardness increases to HV 200. Up to 10% Mg, we can consider that the hardness linearly increases with increasing Mg content. As a possible reason for this observation, the hardness increase is caused by the increase of the Mg content and dislocation density as well as the decrease of the crystallite size. With the increase of Mg content, the grains become finer and the dislocation density is increased which causes the increase of microhardness. Moreover, the existence of Al_2O_3 particles stacked to Al−Mg matrix causes high internal strains in the matrix due to their high hardness and deformation resistance. For 20% Mg, the observed curve is also increased in a lower slope than that observed for the first stages. That may be due to the steady state in the milling stage. During this stage, the fracture rate of the particles is decreased as shown in Fig. 4(d).

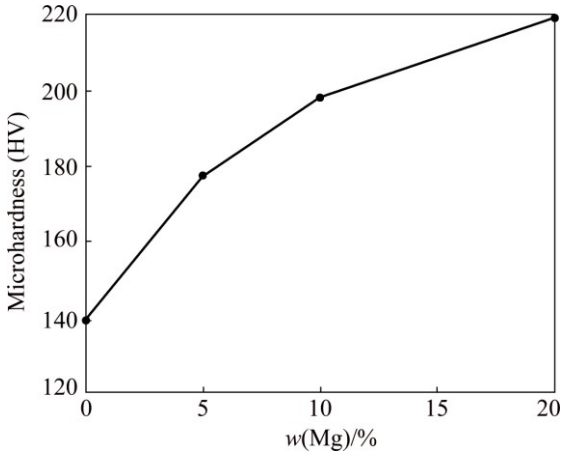

Fig. 6 Microhardness of Al−Mg/5%Al_2O_3 nanocomposite powder after 20 h milling with different Mg contents (0, 5%, 10% and 20%)

Finally, the strength of nano-crystalline solid solutions depends upon both solid solution hardening and grain-boundary hardening [24]. Therefore, the microhardness of the composite depends on both parameters, i.e., the solid solution hardening and the change in the grain size. So, in the introduced composite, the Mg addition forms a solid solution of Al−Mg which forms a smaller grain size and the total effect is hardening and increase of the composite hardness. By the contrary, if the solute addition causes the grain size to increase, the result is softening of the composite.

3.4 Electrical and thermal conductivity

Figure 7 shows the relationship between the thermal conductivity and the temperature. The relation between electrical resistivity and temperature can be extrapolated from the figure. Figure 7 shows that the thermal conductivity increases monotonically with increasing

temperature. Adding reinforcement, such as Al_2O_3, to pure metal, such as Al, reduces its electrical and thermal conductivities due to the fact that the electrical and thermal conductivities for Al_2O_3 are very small compared with their values for Al [18]. However, it is noted that the thermal conductivity of Al−5%Al_2O_3 nanocomposite increased with increasing temperature. The thermal conductivity of a metal can be expressed by the sum of two terms; the residual component and the thermal one. The residual component is caused by structural imperfections such as dislocations, grain boundaries, and impurities and is almost independent of temperature [25]. The thermal component is mainly dependent on the thermal energy applied to the composite. As it is well known, the thermoelectrical conductivity depends mainly on the movement of electrons. As the thermal energy increases, the number of free electrons increases which in turn increases the thermal conductivity. In quantum theory, only electrons which are close to the Fermi energy level are expected to participate in electrical conduction. For Al−Mg/5%Al_2O_3 nanocomposite, the thermal conductivity of the composites is affected by the residual component and the thermal one.

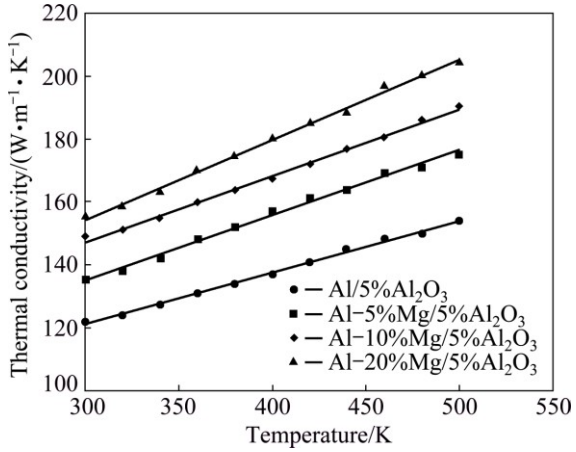

Fig. 7 Variation of thermal conductivity for Al−Mg/5%Al_2O_3 nanocomposites with different Mg contents

The relation between the thermal conductivity and temperature can be fitted with a linear equation as follows:

$$k=AT+B \quad (4)$$

where k is the thermal conductivity; T is the temperature; A and B are two parameters depending on the composite components. The values for A and B for different Mg contents are shown in Table 2.

Figure 8 shows the effect of Mg content on the thermal conductivity of the prepared samples. The thermal conductivity increases by increasing the Mg content. The measured thermal conductivities of Al−Mg/5%Al_2O_3 nanocomposites are 122.2, 138.4, 149.5, and 155.8 W/(m·K) for the 0, 5%, 10% and 20% Mg, respectively. There are two reasons for this increase: 1) the fact that the thermal conductivity of Mg is 5 times greater than that for Al_2O_3 and 2) the movement of electrons is affected by structural imperfections existing in the composites. Additionally, the increasing rate in the small Mg content is larger than that for the large Mg content, this can be due to the steady state at 20% Mg.

Table 2 A and B values for different Mg contents

w(Mg)/%	A	B
0	0.164	71.92
5	0.206	73.19
10	0.212	83.69
20	0.255	77.92

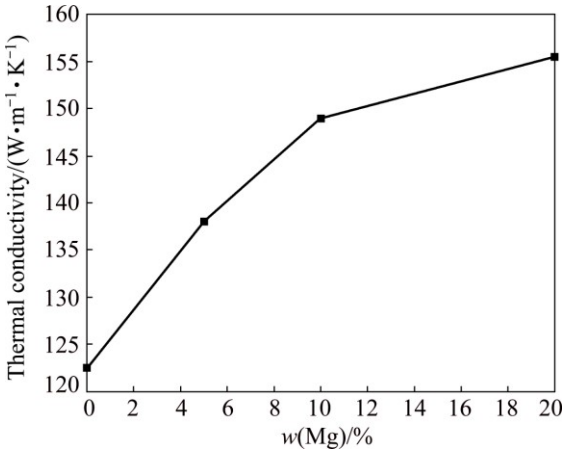

Fig. 8 Effect of Mg content on thermal conductivity of Al−Mg/5%Al_2O_3 nanocomposite

4 Conclusions

1) Milling of Al−Mg/5%Al_2O_3 for 20 h causes the formation of the FCC supersaturated $Al(Mg)_{ss}$ due to the Mg atomic penetration into the substitution sites of the Al lattice.

2) The crystallite size is decreased by increasing Mg content, it decreases from 43 to 27 nm with increasing Mg content from 0 to 20% in the composite. By the contrary, the lattice strain is increased from 0.22% to 0.325% after 20 h milling. This is due to the diffusion of Mg atoms in the Al lattice which increases dislocation density and leads to the grain refinement and accumulation of internal strain in the matrix.

3) By increasing the Mg content from 0 to 20% in the composite, a noticeable change in the particles shape and size is observed, the average particle size diminishes from 30 to 5 μm at 20 Mg% composite.

4) Microhardness of the milled powder increases with the increase of Mg content. This enhancement in the hardness is caused by the dislocation density and the

reduction in the crystallite size caused by not only the diffusion of Mg atoms in Al matrix but also, the existence of Al_2O_3 hard particles.

5) The thermal conductivity increases monotonically with increasing temperature for all inspected composites. The relation between thermal conductivity and temperature can be expressed in a linear function with two parameters dependent on the composite constituents. As the thermal energy increases, the number of free electrons increases which in turn increases the thermal conductivity. Also, as the Mg content increases, the thermal conductivity of the composite increases. That is due to the fact that the thermal conductivity of Mg is larger than that of Al_2O_3 and the moving electrons are affected by the dislocation density and structural imperfections.

References

[1] CLYNE T, WITHERS P. An introduction to metal matrix composites [M]. Cambridge, UK: Cambridge University Press, 1993.

[2] MIRACLE D B. Metal matrix composites−from science to technological significance [J]. Composites Science & Technology, 2005, 65: 2526−2540.

[3] FOGAGNOLO J B, VELASCO F, ROBERT M H, TORRALBA J M. Effect of mechanical alloying on the morphology, microstructure and properties of aluminum matrix composite powders [J]. Materials Science and Engineering A, 2003, 342: 131−143.

[4] KHAKBIZ M, AKHLAGHI F. Synthesis and structural characterization of Al−B_4C nano-composite powders by mechanical alloying [J]. Journal of Alloys and Compounds, 2009, 479(1): 334−341.

[5] LIU Y, CONG H, WANG W, SUN C, CHENG H. Al nanoparticle-reinforced nanocrystalline Al matrix composites: Fabrication and mechanical properties [J]. Materials Science and Engineering A, 2009, 505(1): 151−156.

[6] WAGIH A. Experimental and finite element simulation of nano-indentation on metal matrix composites: Hardness prediction [J]. International Journal of Engineering, 2016, 29(1): 78−86.

[7] PRABHU B, SURYANARAYANA C, AN L, VAIDYANATHAN R. Synthesis and characterization of high volume fraction Al−Al_2O_3 nanocomposite powders by high-energy milling [J]. Materials Science and Engineering A, 2006, 425: 192−200.

[8] WAGIH A. Synthesis of nanocrystalline Al_2O_3 reinforced Al nanocomposites by high-energy mechanical alloying: Microstructural evolution and mechanical properties [J]. Transactions of the Indian Institute of Metals, 2016, 69(4): 851−857.

[9] LU L, ZHANG Y. Influence of process control agent on interdiffusion between Al and Mg during mechanical alloying [J]. Journal of Alloys and Compounds, 1999, 290: 279−283.

[10] WAGIH A. Effect of milling time on morphology and microstructure of Al−Mg/Al_2O_3 nanocomposite powder produced by mechanical alloying [J]. Int J Adv Eng Sci, 2014, 4(2): 1−7.

[11] GUBICZA J, KASSEM M, RIBARIK G T U. The microstructure of mechanically alloyed Al−Mg determined by X-ray diffraction peak profile analysis [J]. Materials Science and Engineering A, 2004, 372: 115−122.

[12] ZEBARJAD S M, SAJJADI S A. Microstructure evaluation of Al−Al_2O_3 composite produced by mechanical alloying method [J]. Materials and Design, 2006, 27: 684−688.

[13] WAGIH A. Mechanical properties of Al−Mg/Al_2O_3 nanocomposite powder produced by mechanical alloying [J]. Advanced Powder Technology, 2015, 26: 253−258.

[14] CHEN Y S, CHEN T J, ZHANG S Q, LI P B. Effect of ball milling on microstructural evolution during partial remelting of 6061 aluminum alloy prepared by cold-pressing of alloy powders [J]. Transactions of Nonferrous Metals Society of China, 2015, 25(7): 2113−2121.

[15] SAFARI J, AKBARIA G H, SHAHBAZKHAN A, DELSHAD CHERMAHINI M. Microstructural and mechanical properties of Al−Mg/Al_2O_3 nanocomposite prepared by mechanical alloying [J]. Journal of Alloys and Compounds, 2011, 509: 9419−9424.

[16] RAJKOVIC V, BOZIC D, MILAN T J. Effects of copper and Al_2O_3 particles on characteristics of Cu−Al_2O_3 composites [J]. Materials and Design, 2010, 31: 1962−1970.

[17] FANG W B, LI X W, SUN H F, DING Y F. Characterization of Ti−50Al composite powder synthesized by high energy ball milling [J]. Transactions of Nonferrous Metals Society of China, 2011, 21(S): s333−s337.

[18] TATAR C, ÖZDEMIR N. Investigation of thermal conductivity and microstructure of the α-Al_2O_3 particulate reinforced aluminum composites (Al/Al_2O_3-MMC) by powder metallurgy method [J]. Physica B: Condensed Matter, 2010, 405(3): 896−899.

[19] WILLIAMSON G, HALL W. X-ray line broadening from filed aluminium and wolfram [J]. Acta Metal, 1953, 1: 22−31.

[20] CRIVELLO J C, NOBUKI T, KUJI T. Limits of the Mg−Al γ phase range by ball-milling [J]. Intermetallics, 2007, 15: 1432−1437.

[21] FRANZ R, WIEDEMANN G. Ueber die wa¨rme-leitungsfa¨higkeit der metalle [J]. Annalen der Physik, 1853, 165(8): 497−531.

[22] SCUDINO S, SAKALIYSKA M, SURREDDI K B, ECKERT J. Mechanical alloying and milling of Al−Mg alloys [J]. Journal of Alloys and Compounds, 2009, 483: 2−7.

[23] ZHAO L, ZWICK J, LUGSCHEIDER E. The influence of milling parameters on the properties of the milled powders and the resultant coatings [J]. Surface and Coatings Technology, 2003, 168: 179−185.

[24] KOCH C C, OVIDKO I A, SEAL S, VEPREK S. Structural nanocrystalline materials: Fundamentals and applications [M]. Cambridge, UK: Cambridge University Press, 2007: 141−145.

[25] KIM Y D, OH N L, OH S T, MOON I H. Thermal conductivity of W−Cu composites at various temperatures [J]. Materials Letters, 2001, 51(5): 420−424.

添加 Mg 对 $Al-Al_2O_3$ 纳米复合材料力学性能和热电性能的影响

A. WAGIH

Mechanical Design and Production Dept, Faculty of Engineering,
Zagazig University, P. O. Box 44519, Zagazig, Sharkia, Egypt

摘　要：采用机械合金化制备不同 Mg 含量(0，5%，10%，20%)的 $Al-Mg/5\%Al_2O_3$ 纳米复合材料，研究 Mg 含量对材料力学和热电性能的影响。采用扫描电子显微镜、X 射线衍射和透射电子显微镜对所得粉末进行表征。结果表明，往 $Al-Al_2O_3$ 复合材料中添加 Mg 可形成 Al−Mg 固溶体。随着 Mg 含量的增加，Al 的点阵位置逐渐被 Mg 取代，导致晶粒尺寸减小，晶格应变增加。随着 Mg 含量的增加，复合材料的显微硬度增加。热导率和电导率随着温度升高线性增加。热导率随 Mg 含量的增加而增加。

关键词：$Al-Al_2O_3$ 纳米复合材料；Mg；机械合金化；显微硬度；热电性能

(Edited by Xiang-qun LI)